ISSN 1063-7834, Physics of the Solid State, 2020, Vol. 62, No. 7, pp. 1145–1149. © Pleiades Publishing, Ltd., 2020.
Russian Text © The Author(s), 2020, published in Fizika Tverdogo Tela, 2020, Vol. 62, No. 7, pp. 1017–1021.

SUPERCONDUCTIVITY

# Magnetization Anisotropy in the Textured Bi-2223 HTS in Strong Magnetic Fields

**D. M. Gokhfeld[a, b, *] and D. A. Balaev[a, b]**

[a] *Kirensky Institute of Physics, Krasnoyarsk Scientific Center, Siberian Branch, Russian Academy of Sciences, Krasnoyarsk, 660036 Russia*

[b] *Siberian Federal University, Krasnoyarsk, 660041 Russia*

**e-mail: gokhfeld@iph.krasn.ru*

Received February 13, 2020; revised February 13, 2020; accepted February 18, 2020

**Abstract**—The origin of the low magnetization anisotropy of the textured bulk samples consisting of highly anisotropic $(Bi,Pb)_2Sr_2Ca_2Cu_3O_x$ (Bi-2223) high-temperature superconductor crystallites has been investigated. It has been established that the observed anisotropy is determined by the disordering of Bi-2223 crystallites in the sample. The measured anisotropy of the textured sample makes it possible to determine the magnetic angle characterizing the ordering of crystallites.

**Keywords:** critical current, anisotropy, magnetization hysteresis loop, BSCCO

**DOI:** 10.1134/S1063783420070069

## 1. INTRODUCTION

The significant anisotropy of the physical properties of high-temperature superconductor (HTS) crystals is related to their layered crystalline structure. In HTS single crystals, the anisotropy of the critical current in the *ab* plane is negligible, in contrast to the high anisotropy of the properties relative to the *c* axis direction and in the *ab* plane. The anisotropy of a superconducting crystal is determined by the coefficient $\gamma = J_{c,\,ab}/J_{c,\,c}$, where $J_{c,\,ab}$ is the critical current density in the *ab* plane and $J_{c,\,c}$ is the critical current density along the crystal *c* axis. The $(Bi,Pb)_2Sr_2Ca_2Cu_3O_x$ (Bi-2223) HTS is known for its highest anisotropy; the coefficient $\gamma$ in it exceeds 150 [1, 2].

In polycrystalline HTSs, the disordering of anisotropic crystallites (hereinafter, crystallite means a laminated grain, a microcrystal) leads to a decrease in the transport critical current density. The creation of an ordered crystallite structure (texture) in a polycrystalline HTS makes it possible to increase the critical transport current by bringing its density closer to $J_{c,\,ab}$ [3]. However, in the textured Bi-2212 and Bi-2223 superconductors, the anisotropy value determined by the transport and magnetic measurements [4–7] is merely 2–5, which is much lower than the anisotropy values for single crystals.

The anisotropy of the magnetic properties of a textured superconductor is mainly determined by the internal crystalline anisotropy. The measured anisotropy value can depend on the sample or grain shape and on the disordering of crystallites.

In this study, we investigate the effect of different mechanisms on the anisotropy of the magnetic properties and clarify the origin of the low anisotropy of bismuth-based textured HTSs. To do that, we analyze the magnetization hysteresis loops of the textured Bi-2223 HTS that were reported previously in [8, 9].

## 2. MAGNETIC ANISOTROPY OF THE TEXTURED Bi-2223 HTS

Samples for the magnetization measurements were cut in the form of cubes with 1.6-mm faces. Two orientations of the external magnetic field *H* relative to the preferred crystallite direction in the textured sample were used: (i) the magnetic field perpendicular to the texturing plane ($H \parallel c$) and the magnetic field directed along the texturing plane ($H \parallel ab$). The magnetization *M* of textured Bi-2223 was measured in the magnetic field range of ±6 T at temperatures from 4.2 to 80 K [9]. For silver-added textured Bi-2223 [8], the measurements were performed in fields of ±6 T at 4.2 K and ±0.15 T at 80 K.

The insets in Figs. 1a and 1b show the Bi-2223 magnetization hysteresis loops for the external field oriented perpendicular and parallel to the texturing plane. The hysteresis loops have features typical of the magnetization curves of non-hard type-II superconductors. The axial asymmetry relative to the *H* axis increases with temperature. The maximum diamagnetic response is obtained in the external magnetic field approximately equal to the complete penetration field. The complete penetration field is the external

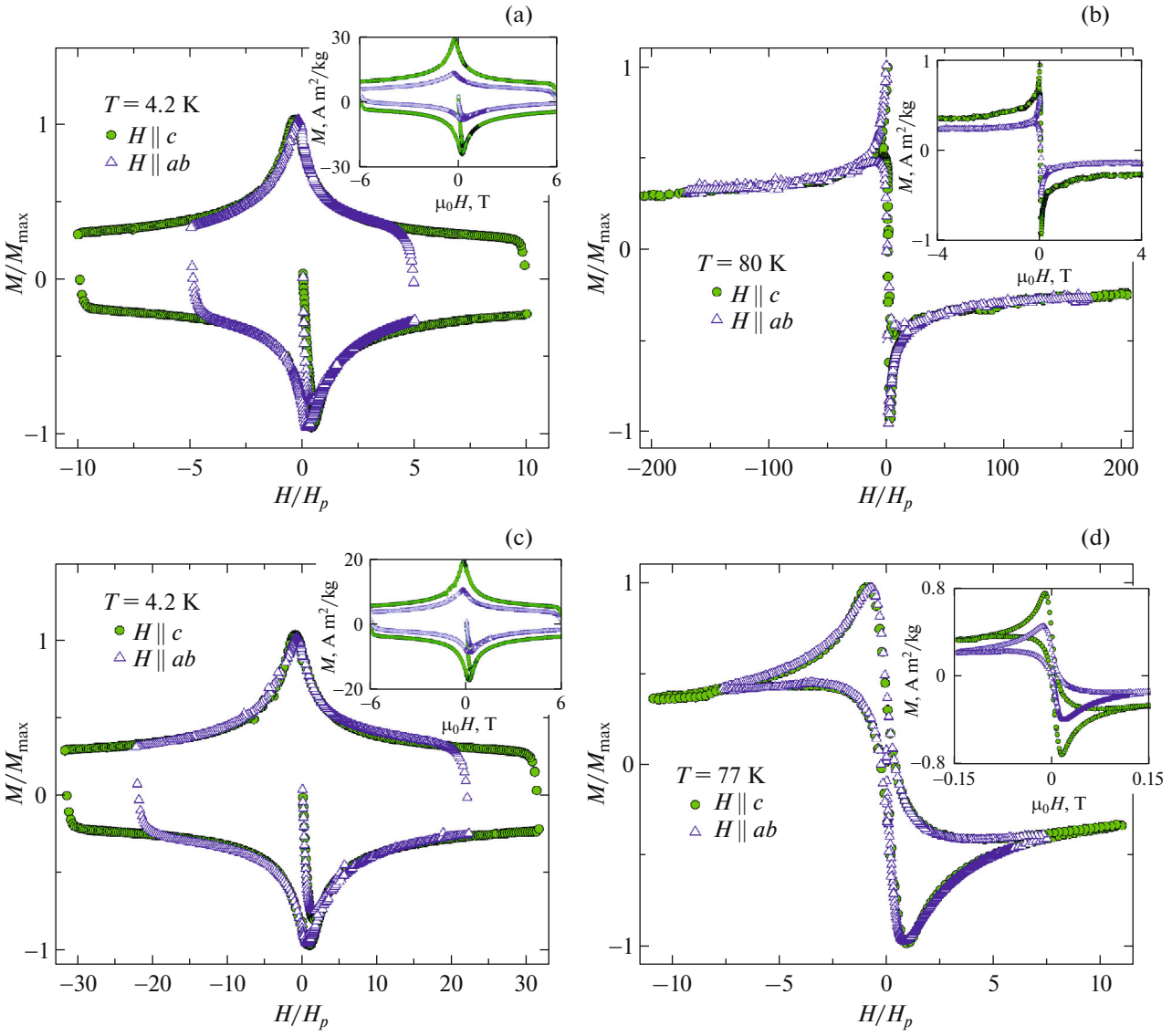


**Fig. 1.** (a, b) Magnetic hysteresis of Bi-2223 at **H** ∥ *c* and **H** ∥ *ab*. (c, d) Scaling of the magnetization hysteresis loop of textured Bi-2223. Insets: hysteresis loops at different orientations of the external magnetic field.

field at which the initial magnetization portion and the full hysteresis loop merge. As the temperature $T$ increases from 4.2 to 80 K, the complete penetration field $H_{p,\ H \parallel c}$ exponentially decreases from 0.6 to 0.01 T and the field $H_{p,\ H \parallel ab}$ changes from 1.2 to 0.02 T (hereinafter, the subscript $H \parallel c$ or $H \parallel ab$ indicates the orientation of the external field relative to the sample texturing plane). The analogous exponential decrease with temperature was noticed for the critical current density [9]. Similarly, in the same temperature range, the absolute value of the maximum diamagnetic response decreases: $M_{\max,\ H \parallel c}$ decreases from 26.5 A m$^2$/kg to 1.2 A m$^2$/kg and $M_{\max,\ H \parallel ab}$, from 10.9 A m$^2$/kg to 0.6 A m$^2$/kg.

## 3. ANALYSIS

### *3.1. Scaling of the Magnetization Curves*

The effect of the orientation of an anisotropic superconductor in an external magnetic field on the thermodynamic parameters is successfully described by the Ginzburg–Landau theory of anisotropic superconductors [10]. The magnetic field orientation-dependent parameters of an anisotropic crystal can be associated with the parameters of an equivalent isotropic crystal in the effective field $H^*$. The effective field $H^*$ is determined as

$$H^* = H(\gamma^{-2}\sin^2\theta + \cos^2\theta)^{0.5}, \qquad (1)$$

where θ is the angle between the external field direction and the crystal $c$ axis. According to [11], the field

dependences of the magnetization of the anisotropic sample at $H \parallel c$ and $H \parallel ab$ are related as

$$M_{H\|c}(H) = \gamma M_{H\|ab}(\gamma H). \quad (2)$$

Scaling relation (2) is used to determine the anisotropy coefficient $\gamma$ from the magnetic measurements.

Figures 1a and 1b show the hysteresis loops of the magnetization of textured Bi-2223 at $T = 4.2$ K and 80 K in the coordinates $M/M_{\max}$ vs $H/H_p$. In these coordinates, the magnetization curves at $H \parallel c$ and $H \parallel ab$ coincide. As the temperature increases, the $M_{\max}$ and $H_p$ values decrease. However, the ratio $H_{p,\,H\parallel ab/p,\,H\parallel c} = 2.0 \pm 0.3$ does not change at all temperatures. The ratio $M_{\max,\,H\parallel c}/M_{\max,\,H\parallel ab}$ slightly decreases (from 2.5 to 2.2) with an increase in temperature from 4.2 to 80 K. Scaling relation (2) satisfactorily describes the effect of the external magnetic field orientation on the magnetization at a sufficiently small coefficient of $\gamma \approx 2$–2.5. The similar behavior of the magnetization hysteresis loops is observed for silver-added textured Bi-2223. Figures 1c and 1d show the scaling of the $M(H)$ hysteresis loops at temperatures of 4.2 and 77 K. In this material, the estimated anisotropy coefficient appeared to be even lower: $\gamma \approx$ 1.4–1.7.

It should be noted that the comparable low anisotropy values were obtained previously in studying the magnetoresistance of the same materials [7, 12]. Although the magnetoresistance of granular HTSs is determined, to a great extent, by grain boundaries [13–16], in highly anisotropic HTSs, including Bi-2223, the dissipation inside grains occurs also in moderate and strong magnetic fields [12, 17, 18]. When the external field is directed perpendicular to the texturing plane ($H \parallel c$), the resistance is higher than at the field orientation parallel to the texturing plane ($H \parallel ab$) by a factor of approximately 2.4. Thus, the anisotropy determined from the magnetization hysteresis loops and from the magnetoresistance of the textured samples appears to be much lower than the anisotropy of the Bi-2223 crystal.

### *3.2. Effect of the Crystallite Shape on the Magnetic Anisotropy*

The magnetization anisotropy depends also on the superconductor sizes in the directions parallel and perpendicular to the applied magnetic field. According to the critical state model [19], the magnetization of the sample is proportional to the density of the critical current circulating in the plane perpendicular to the magnetic field. For an anisotropic superconductor, the modification of the critical state model was proposed in [20]. At $H \parallel ab$, the height of the magnetization hysteresis $\Delta M$ of an anisotropic crystal is determined from the formulas

$$\Delta M_{H\|ab} = J_{c,ab}\frac{d}{2}\left(1 - \frac{d}{3l}\frac{J_{c,ab}}{J_{c,c}}\right) \quad (3)$$
$$\text{at} \quad J_{c,ab}/J_{c,c} < l/d$$

and

$$\Delta M_{H\|ab} = J_{c,c}\frac{l}{2}\left(1 - \frac{l}{3d}\frac{J_{c,c}}{J_{c,ab}}\right) \quad (4)$$
$$\text{at} \quad J_{c,ab}/J_{c,c} > l/d > 1,$$

where $d$ is the crystal thickness along the $c$ axis and $l$ is the minimum crystal size in the $ab$ plane. At $H \parallel c$, the current circulates in the $ab$ plane and the loop height is determined as

$$\Delta M_{H\|c} = J_{c,ab} l/3. \quad (5)$$

Let us estimate the magnetization anisotropy, which should correspond to the anisotropy of the Bi-2223 crystal. The textured ceramic under study consists of ordered flat crystallites with a thickness of ~1 μm along the $c$ axis and lateral sizes of ~5–10 μm in the $ab$ plane [8, 9]. The magnetization of a polycrystalline sample is determined by the circulation of currents on the grain scale [21, 22]; therefore, the crystallite sizes should be substituted into formulas (3–5). We take $l \approx 7$ μm, $d \approx 1$ μm, and $J_{c,\,ab}/J_{c,\,c} > 150$, so $J_{c,\,ab}/J_{c,\,c} > l/d$. Using formulas (4) and (5), we express the magnetization anisotropy as

$$\frac{\Delta M_{H\|c}}{\Delta M_{H\|ab}} = \frac{2}{3}\frac{J_{c,ab}}{J_{c,c}}\left(1 - \frac{l}{3d}\frac{J_{c,c}}{J_{c,ab}}\right)^{-1}. \quad (6)$$

Substituting the sizes and critical current densities of crystallites, we obtain $\Delta M_{H\,\|\,c}/\Delta M_{H\,\|\,ab} > 101$. However, the Bi-2223 magnetization hysteresis loops (Fig. 1a) have a much smaller ratio between the hysteresis heights: $\Delta M_{H\,\|\,c}/\Delta M_{H\,\|\,ab} \approx 2.5$. Thus, the laminated shape of crystallites does not explain the observed anisotropy of the magnetization of the textured sample.

### *3.3. Effect of Crystallite Disordering*

The imperfect ordering of crystallites in a textured sample is equivalent to the deviation of the external magnetic field from the selected directions 0 and 90° in an anisotropic superconducting crystal. Let us consider how this deviation affects the magnetization hysteresis loop and the $H_p$ value. Figure 2 shows a schematic of the sample consisting of ordered laminated crystallites (on the left) and the magnetic response of an anisotropic superconducting crystal in an oblique field (on the right). $M_c$ is the magnetization induced by the currents circulating in the $ab$ plane. $M_{ab}$ is the magnetization induced by the currents circulating perpendicular to the crystal $ab$ plane. Then, we assume

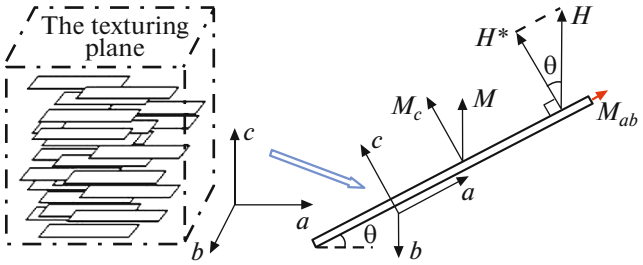


**Fig. 2.** Schematic of the magnetic response of the anisotropic crystallite rotated by angle θ relative to the texturing plane. The orientation of the *a*, *b*, and *c* axes of the crystallite differs from the orientation of the axes of the textured sample. The case of the external field orientation $H \parallel ab$ relative to the sample axes is illustrated.

$M_{ab} \ll M_c$, so that the magnetization $M_{ab}$ can be ignored (the high anisotropy). Indeed, in highly anisotropic superconductors, the currents flow mainly along the crystallite *ab* planes [7, 23–25]. Hence, the magnetization of a superconductor is determined by the circulation of the currents in the crystallite *ab* planes.

In the measurements, the projection of the magnetization onto the axis corresponding to the field direction is determined. At the same time, the currents induced in the *ab* plane depend on the projection of the field *H* onto the *c* axis. For the anisotropic plate shown in Fig. 2, the measured magnetization is lower than the magnetization in the direction parallel to the plate *c* axis: $M_{H \parallel c} = M_c \cos\theta$ and $M_{H \parallel ab} = M_c \sin\theta$. The projection of the field *H* onto the *c* axis is $H^*_{H\|c} = H\cos\theta$ and $H^*_{H\|ab} = H\sin\theta$. Consequently, we have the relation $M_{H \parallel c}(H\cos\theta)/\cos\theta = M_{H \parallel ab}(H\sin\theta)/\sin\theta$, which can be written in the form

$$M_{H\|c}(H) = k_\gamma M_{H\|ab}(k_\gamma H), \qquad (7)$$

where $k_\gamma = \cot\theta$.

We define the magnetic disordering angle θ* as the absolute value-averaged deviation of crystallites from the texturing plane in a textured polycrystalline superconductor [26]. Scaling formula (7) with $k_\gamma = \cot\theta^*$ describes the relation between the field dependences of the magnetization of the textured sample at $H \parallel c$ and $H \parallel ab$. Note that formula (7) coincides with scaling formula (2) for $k_\gamma = \gamma$, although the magnetization anisotropy has different origins. The magnetic angle θ* characterizes the disordering of crystallites. A disordered polycrystalline sample has θ* = 45°. In the textured sample with θ* < 1°, the effect of the internal anisotropy of crystallites is no longer negligible. At θ* = 0, the divergence of formula (7) arises, which is related to the used high anisotropy approximation $\gamma = \infty$.

Scaling for textured Bi-2223 with $k_\gamma = 2.5$ (the data in Figs. 1a, 1b) corresponds to a magnetic angle of θ* = 21.8°. Such a significant value is indicative of the dispersion of the crystallite orientation distribution in the investigated material [27]. Scaling for textured Bi-2223 + Ag with $k_\gamma = 1.7$ (the data in Figs. 1c, 1d) corresponds to a magnetic angle of θ* = 30.5°. In this sample, crystallites are less ordered than in the textured Bi-2223 sample (at θ* = 21.8°). The imperfect crystallite ordering weakens the diamagnetic signal in the samples under study. It should be noted that the Lotgering factor [28] obtained from the X-ray diffraction patterns of the samples is 0.97 ± 0.01 [8]. Such a value corresponds to a magnetic angle of ~1° and a high degree of ordering [27]. The difference between the degrees of ordering obtained from the X-ray diffraction and magnetic data can be caused by the dependence of the crystallite orientation distribution on the distance from the sample surface. The high ordering of crystallites was apparently implemented only on the surface of the investigated samples, while the crystallite orientation in the bulk is less ordered. The creation of superconducting ribbons with highly ordered Bi-2223 crystallites makes it possible to obtain materials with a magnetization anisotropy of more than 20 and the improved conductive properties [29, 30].

For the investigated samples, the best agreement between the field dependences at different temperatures is obtained at slightly different scaling coefficients for the abscissa and ordinate axes: $M_{\max,\, H \parallel c}/M_{\max,\, H \parallel ab} \approx 2.5$ and $H_{p,\, H \parallel ab}/H_{p,\, H \parallel c} \approx 2$ (Figs. 1a, 1b). The difference between the scaling coefficients for the abscissa and ordinate axes can be explained by a special structure of Abrikosov vortices in a layered superconductor. The magnetic vortices in HTSs are pancake vortices [31]. In the oblique field, the cores of the pancake vortices can shift in different layers of an HTS crystal, which can decrease the angle between the external field and the vortex filaments in a sample.

### *3.4. Circulation Radius*

The consideration presented in Subsection 3.3 is applicable if currents circulate in the crystallite *ab* planes. In this case, the current circulation scale should be independent of the external magnetic field orientation. The characteristic current circulation scale is estimated from the extended critical state model [21]. According to this model, the asymmetry of the lower and upper branches of the hysteresis loop is related to the ratio between the depth of the surface region with the equilibrium magnetization and the screening current circulation radius $R_c$. The corresponding expression was derived in [22]: $\lambda/R_c \approx 1 - |\Delta M(H_p)/2M\uparrow(H_p)|^{1/3}$, where $\Delta M = M\downarrow - M\uparrow$, $M\uparrow$, and $M\downarrow$ are the magnetizations at the increasing and decreasing external magnetic field and λ is the magnetic field penetration depth. Using the asymmetry of

the magnetization hysteresis loops in Fig. 1a, we found a value of $\lambda/R_c \approx 0.045$ for any sample orientation. The identical asymmetry evidences for the fact that the scale of current circulation in the sample at $H \parallel c$ and $H \parallel ab$ is the same. At $\lambda = 150$ nm [3], we obtain the estimate ~5 μm. This scale corresponds to the size of crystallites in the *ab* plane. Thus, in strong fields, the current circulation occurs mainly in the *ab* planes of individual crystallites for both the $H \parallel c$ and $H \parallel ab$ orientation. Therefore, for any investigated orientation, the magnetization of the textured sample is determined by the projection of the magnetic response of the currents circulating in the *ab* planes of imperfectly ordered crystallites (Fig. 2). In [32], the decisive effect of vortex pinning in the crystallite *ab* plane on the magnetic properties of Bi-2223 ribbons was established.

## 4. CONCLUSIONS

Our analysis showed that, regardless of the external magnetic field orientation, the current circulation occurs in the *ab* plane of Bi-2223 crystallites. The observed anisotropy of the magnetic hysteresis of the textured Bi-2223 samples yields information about the disordering of Bi-2223 crystallites, rather than about their internal anisotropy. A method for determining the effective degree of texturing from the magnetic hysteresis measured at $H \parallel c$ and $H \parallel ab$ was proposed. A significant increase in the diamagnetic response at $H \parallel c$ can be obtained by optimizing the ordering of crystallites in the sample.

## CONFLICT OF INTEREST

The authors declare that they have no conflicts of interest.

## REFERENCES


1. J. C. Martínez, S. H. Brongersma, A. Koshelev, B. Ivlev, P. H. Kes, R. P. Griessen, D. G. de Groot, Z. Tarnavski, and A. A. Menovsky, Phys. Rev. Lett. **69**, 2276 (1992).
2. O. V. Kharissova, E. M. Kopnin, V. V. Maltsev, N. I. Leonyuk, L. M. Leon-Rossano, I. Yu. Pinus, and B. I. Kharisov, Crit. Rev. Solid State **39**, 253 (2014).
3. G. Wang, M. J. Raine, and D. P. Hampshire, Supercond. Sci. Technol. **30**, 104001 (2017).
4. A. D. Caplin, L. F. Cohen, M. N. Cuthbert, M. Dhalle, D. Lacey, G. K. Perkins, and J. V. Thomas, IEEE Trans. Appl. Supercond. **5**, 1864 (1995).
5. G. C. Han, Phys. Rev. B **52**, 1309 (1995).
6. G. C. Han and C. K. Ong, Phys. Rev. B **56**, 11299 (1997).
7. D. M. Gokhfeld, D. A. Balaev, S. V. Semenov, and M. I. Petrov, Phys. Solid State **57**, 2145 (2015).
8. M. I. Petrov, I. L. Belozerova, K. A. Shaikhutdinov, D. A. Balaev, A. A. Dubrovskii, S. I. Popkov, A. D. Vasil'ev, and O. N. Mart'yanov, Supercond. Sci. Technol. **21**, 105019 (2008).
9. D. M. Gokhfeld, D. A. Balaev, M. I. Petrov, S. I. Popkov, K. A. Shaykhutdinov, and V. V. Val'kov, J. Appl. Phys. **109**, 033904 (2011).
10. J. R. Clem, Supercond. Sci. Technol. **11**, 909 (1998).
11. Z. Hao and J. R. Clem, Phys. Rev. B **46**, 5853 (1992).
12. D. A. Balaev, S. I. Popkov, S. V. Semenov, A. A. Bykov, K. A. Shaykhutdinov, D. M. Gokhfeld, and M. I. Petrov, Phys. C (Amsterdam, Neth.) 470, 61 (2010).
13. D. A. Balaev, S. I. Popkov, E. I. Sabitova, S. V. Semenov, K. A. Shaykhutdinov, A. V. Shabanov, and M. I. Petrov, J. Appl. Phys. **110**, 093918 (2011).
14. S. V. Semenov, D. A. Balaev, M. A. Pochekutov, and D. A. Velikanov, Phys. Solid State **59**, 1291 (2017).
15. D. A. Balaev, S. V. Semenov, and M. A. Pochekutov, J. Appl. Phys. **122**, 123902 (2017).
16. V. V. Derevyanko, T. V. Sukhareva, and V. A. Finkel', Phys. Solid State **60**, 470 (2018).
17. D. A. Balaev, A. A. Bykov, S. V. Semenov, S. I. Popkov, A. A. Dubrovskii, K. A. Shaikhutdinov, and M. I. Petrov, Phys. Solid State **53**, 922 (2011).
18. D. A. Balaev, S. I. Popkov, S. V. Semenov, A. A. Bykov, E. I. Sabitova, A. A. Dubrovskiy, K. A. Shaikhutdinov, and M. I. Petrov, J. Supercond. Nov. Magn. **24**, 2129 (2011).
19. C. P. Bean, Phys. Rev. Lett. **8**, 250 (1962).
20. E. M. Gyorgy, R. B. van Dover, K. A. Jackson, L. F. Schneemeyer, and J. V. Waszczak, Appl. Phys. Lett. **55**, 283 (1989).
21. D. M. Gokhfeld, Phys. Solid State **56**, 2380 (2014).
22. D. M. Gokhfeld, Tech. Phys. Lett. **45**, 1 (2019).
23. J. H. Cho, M. P. Maley, J. O. Willis, J. Y. Coulter, L. N. Bulaevskii, P. Haldar, and L. R. Motowidlo, Appl. Phys. Lett. **64**, 3030 (1994).
24. B. Hensel, G. Grasso, and R. Flükiger, Phys. Rev. B **51**, 15456 (1995).
25. A. Diaz, J. Maza, and F. Vidal, Phys. Rev. B **55**, 1209 (1997).
26. B. Lehndorff, M. Hortig, and H. Piel, Supercond. Sci. Technol. **11**, 1261 (1998).
27. R. Furushima, S. Tanaka, Z. Kato, and K. Uematsu, J. Ceram. Soc. Jpn. **118**, 921 (2010).
28. F. K. Lotgering, J. Inorg. Nucl. Chem. **9**, 113 (1959).
29. A. Lascialfari, S. de Gennaro, A. Peruzzi, and C. Sangregorio, J. Phys. D **31**, 2098 (1998).
30. G. Grasso, M. R. Cimberle, P. Guasconi, I. Pallecchi, and C. Ferdeghini, Supercond. Sci. Technol. **12**, 1108 (1999).
31. R. G. Mints, V. G. Kogan, and J. R. Clem, Phys. Rev. B **61**, 1623 (2000).
32. M. Kiuchi, E. S. Otabe, T. Matsushita, T. Kato, T. Hikata, and K. Sato, Phys. C (Amsterdam, Neth.) **260**, 177 (1996).


*Translated by E. Bondareva*